

# Impact of Quantum Confinement on Subthreshold Swing and Electrostatic Integrity of Ultra-Thin-Body GeOI and InGaAs-OI n-MOSFETs

Chang-Hung Yu, *Student Member, IEEE*, Yu-Sheng Wu, *Student Member, IEEE*,  
Vita Pi-Ho Hu, *Student Member, IEEE*, and Pin Su, *Member, IEEE*

**Abstract**—This paper investigates the electrostatic integrity (EI) of ultra-thin-body (UTB) germanium-on-insulator (GeOI) and InGaAs-OI n-MOSFETs considering quantum confinement (QC) using a derived analytical solution of Schrödinger equation verified with TCAD numerical simulation. Although the electron conduction path of the high-mobility channel device can be far from the frontgate interface due to high channel permittivity, our study indicates that the quantum confinement effect can move the carrier centroid toward the frontgate and, therefore, improve the subthreshold swing (SS) of the UTB device. Since InGaAs, Ge, and Si channels exhibit different degrees of quantum confinement due to different quantization effective mass, the impact of quantum confinement has to be considered when one-to-one comparisons among UTB InGaAs-OI, GeOI, and SOI MOSFETs regarding the subthreshold swing and electrostatic integrity are made.

**Index Terms**—Electrostatic integrity (EI), germanium-on-insulator (GeOI), InGaAs-OI, quantum confinement (QC), subthreshold swing (SS), ultra-thin-body (UTB).

## I. INTRODUCTION

GERMANIUM or other III-V materials such as InGaAs as channel materials have been proposed to enable the mobility scaling for CMOS devices [1]–[3]. Their higher permittivity, however, makes them more susceptible to short-channel effects (SCEs). The ultra-thin-body (UTB) structure with thin buried oxide (BOX) has been suggested to improve the device electrostatic integrity (EI) [2]–[5]. With the scaling of channel thickness, the quantum-confinement (QC) effect may become important for scaled UTB devices especially for Ge and InGaAs devices. Whether the quantum confinement effect will significantly impact the EI of UTB GeOI and InGaAs-OI devices has rarely been known and merits investigation. In this paper, we assess the EI for undoped UTB GeOI and InGaAs-OI n-MOSFETs with thin BOX using an analytical solution of Schrödinger equation [6].

Manuscript received July 1, 2011; accepted August 12, 2011. Date of publication October 6, 2011; date of current version March 9, 2012. This work was supported in part by the National Science Council of Taiwan under contracts NSC 99-2221-E-009-174 and NSC 100-2628-E-009-024-MY2, and in part by the Ministry of Education in Taiwan under ATU program. The review of this paper was arranged by Associate Editor M. P. Anantram.

The authors are with the Department of Electronics Engineering & Institute of Electronics, National Chiao Tung University, Hsinchu 30010, Taiwan (e-mail of corresponding author: pinsu@faculty.nctu.edu.tw).

Color versions of one or more of the figures in this paper are available online at <http://ieeexplore.ieee.org>.

Digital Object Identifier 10.1109/TNANO.2011.2169084

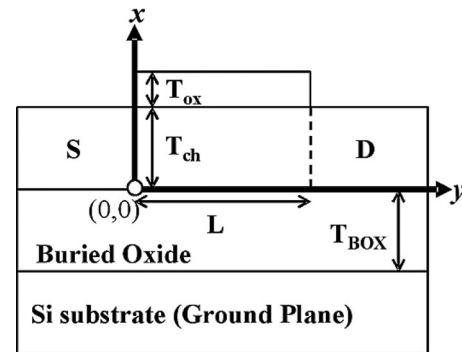


Fig. 1. Schematic sketch of a UTB structure with thin buried oxide (BOX). The origin point is located at the channel/BOX interface of source/channel junction.  $L$  is the channel length.  $T_{ch}$ ,  $T_{ox}$ , and  $T_{BOX}$  are thicknesses of channel, gate oxide, and BOX, respectively.

tion [6]. This paper is organized as follows. In Section II, we present the analytical solution of Schrödinger equation for UTB MOSFETs under the subthreshold region and verify our calculated eigen-energy and subthreshold drain current with TCAD numerical simulation. In Section III, we investigate and compare the impact of quantum confinement on the subthreshold integrity of GeOI and SOI devices. Investigation and comparison of the EI considering the QC effect for UTB InGaAs-OI and GeOI MOSFETs are presented in Section IV. Finally, the conclusions are drawn in Section V.

## II. ANALYTICAL SOLUTION OF SCHRÖDINGER EQUATION

Fig. 1 shows a schematic sketch of a UTB structure with thin buried oxide and ground plane. To consider the quantum-confinement effect along the channel-thickness (i.e.,  $x$ ) direction, the 1-D Schrödinger equation can be expressed as

$$-\frac{\hbar^2}{2m_x} \cdot \frac{d^2\Psi_j(x)}{dx^2} + E_C(x) \cdot \Psi_j(x) = E_j \cdot \Psi_j(x) \quad (1)$$

where  $E_j$  is the  $j$ th eigen-energy,  $\Psi_j$  is the corresponding wavefunction, and  $m_x$  is the carrier quantization effective mass [7], [8]. For long-channel undoped UTB MOSFETs, the conduction band edge  $E_C(x)$  was usually treated as a triangular well in the past [9]. However, to account for the drain-source coupling for short-channel UTB MOSFETs, the conduction band edge  $E_C(x)$  in (1) should be treated as a parabolic well [10] with potential energy  $E_C(x) = \alpha x^2 + \beta x + \gamma$ , where  $\alpha$ ,  $\beta$ ,

and  $\gamma$  are channel-length-dependent coefficients and can be obtained from the channel potential solution of Poisson's equation under subthreshold region [11], [12]. Using the parabolic-well approximation, the solution of (1) can be expressed as [13]

$$\Psi_j = \sum_n d_n \cdot x^n \quad (2a)$$

by using the power series method with the following coefficient  $d_n$ 's:

$$\begin{aligned} d_2 &= -\frac{m_x}{\hbar^2} (E_j - \gamma) \cdot d_0 \\ d_3 &= -\frac{m_x}{3\hbar^2} [(E_j - \gamma) \cdot d_1 - \beta \cdot d_0] \\ d_n &= -\frac{m_x}{n(n-1)\hbar^2} \\ &\times [(E_j - \gamma) \cdot d_{n-2} - \beta \cdot d_{n-3} - \alpha \cdot d_{n-4}], \quad n \geq 4. \end{aligned} \quad (2b)$$

Then the  $j$ th eigen-energy  $E_j$  can be determined by the boundary condition  $\Psi_j(x=0) = \Psi_j(x=T_{ch}) = 0$ , where  $x=0$  and  $x=T_{ch}$  (channel thickness) are defined as the interface positions of BOX/channel and channel/gate-oxide, respectively. Thus, the eigen-energies and wavefunctions of short-channel UTB MOSFETs under subthreshold region can be derived. By using the calculated eigen-energies and wavefunctions, we can calculate the electron density in the channel. The electron density can be expressed as [7]

$$n(x, y) = N_{C,QM}(x, y) \cdot \exp\left(\frac{E_F(y) - E_C(x, y)}{kT}\right) \quad (3a)$$

$$\begin{aligned} N_{C,QM}(x, y) &= \sum_{\nu} \left\{ \frac{d_{\nu} m_{d,\nu} kT}{\pi \hbar^2} \right. \\ &\cdot \left. \sum_j \left[ \exp\left(\frac{E_C(x, y) - E_{j,\nu}}{kT}\right) \cdot |\Psi_{j,\nu}(x, y)|^2 \right] \right\} \end{aligned} \quad (3b)$$

where  $\nu$  is the type of valley,  $d_{\nu}$  is the degeneracy of the valley,  $m_{d,\nu}$  is the corresponding density-of-state effective mass [7], [8], and  $E_F(y)$  is the quasi-Fermi level along the channel-length (i.e.,  $y$ ) direction. In other words, the impact of quantized eigen-energies and wavefunctions on the electron density is incorporated into the effective density-of-state for conduction band ( $N_{C,QM}$ ) [14]. Using  $N_{C,QM}$ , the subthreshold drain current can be derived by [15], [16]

$$I_{DS} = \frac{q\mu_n W (kT/q) [1 - \exp(-qV_{DS}/kT)]}{\int_0^L dy / \int_0^{T_{ch}} N_{C,QM}(x, y) \cdot \exp(-E_C(x, y)/kT) dx} \quad (4)$$

where  $\mu_n$  is the electron mobility,  $W$  is the channel width, and  $kT/q$  is the thermal voltage.

We have verified our model using TCAD numerical simulation that numerically solves the self-consistent solution of 2-D Poisson and 1-D Schrödinger equations [17]. Fig. 2 shows that the eigen-energies  $E_j$ 's calculated by our model are fairly accurate for both short-channel UTB GeOI and InGaAs-OI MOSFETs. In addition, it can be seen from Fig. 3 that our cal-

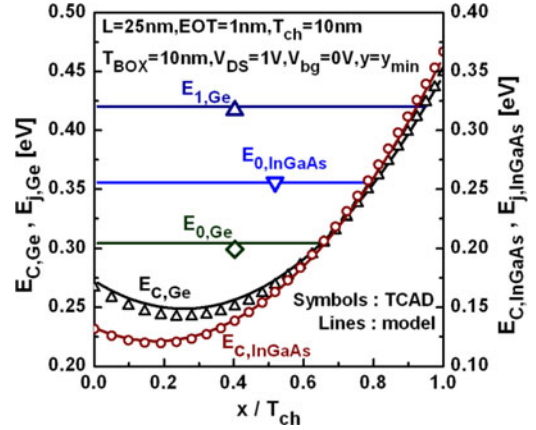


Fig. 2. Conduction band edge and quantized eigen-energies of UTB GeOI and InGaAs-OI MOSFETs for  $V_{DS} = 1$  V and  $V_{GS} = V_{th} - 0.15$  V. 140 terms for (2a) are used in this study.  $y_{min}$  is where the minimum potential occurs for carrier flow along the channel-length direction.

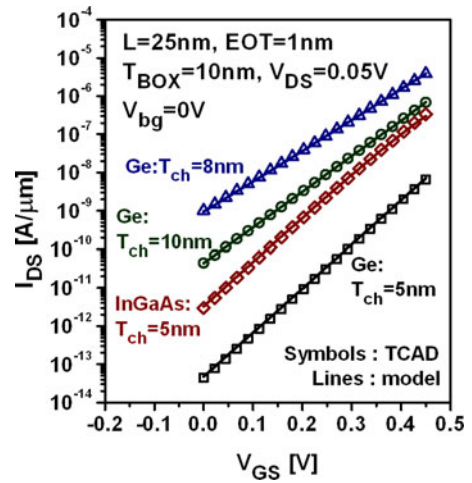


Fig. 3. Calculated subthreshold drain current with various  $T_{ch}$  for GeOI and InGaAs-OI devices considering the QC effect.

culated subthreshold drain current considering the QC effect for various  $T_{ch}$  shows good agreement with the TCAD numerical simulation.

### III. COMPARISON BETWEEN GEOI AND SOI MOSFETs

Fig. 4 shows that, for a given  $T_{ch}$  ( $>6$  nm), the QC effect improves the short-channel subthreshold swing shift [defined as  $SS(L) - SS(L = 100$  nm)] of GeOI and SOI devices. In addition, it can be seen in Fig. 4 that, for a given  $L$ , the impact of quantum confinement on the short-channel subthreshold swing shift of GeOI and SOI devices increases with  $T_{ch}$ . This is because the potential coupling from drain-source becomes stronger with increasing channel thickness. Fig. 5(a) compares the classical (CL) subthreshold swing of UTB GeOI and SOI devices for various channel length ( $L$ ) with  $T_{ch} = 10$  nm. It can be seen that the classical SS of GeOI devices is worse than the SOI one as  $L$  decreases because Ge has higher permittivity than the Si counterpart. In Fig. 5(b), however, when the QC effect is considered, the subthreshold swing of GeOI devices is quite

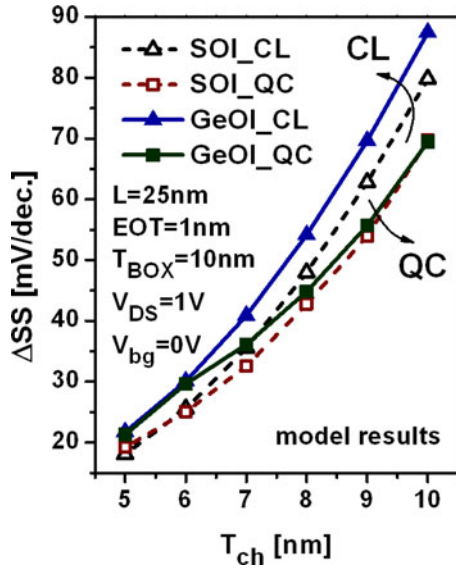


Fig. 4. Impact of channel thickness on the short-channel subthreshold swing shift  $\Delta SS = SS(L) - SS(L = 100 \text{ nm})$  for GeOI and SOI devices.

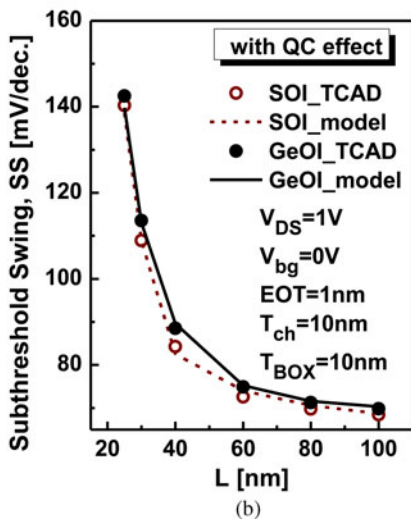
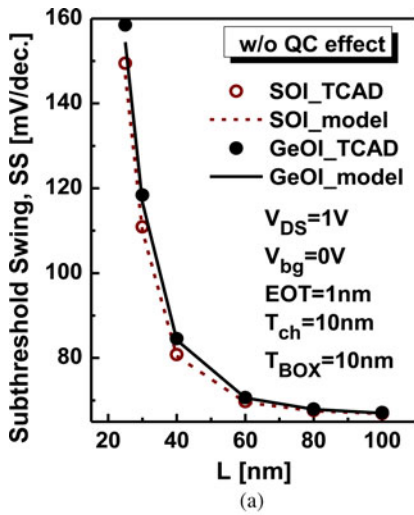


Fig. 5. Comparison of the subthreshold swing of GeOI and SOI devices: (a) without the QC effect, i.e., CL condition, and (b) with the QC effect.

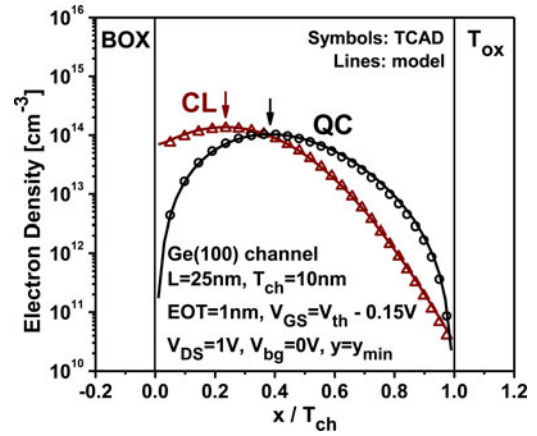


Fig. 6. Electron density distribution for the GeOI device in the subthreshold region with  $T_{ch} = 10 \text{ nm}$ . The arrow tip indicates the electron conduction path.

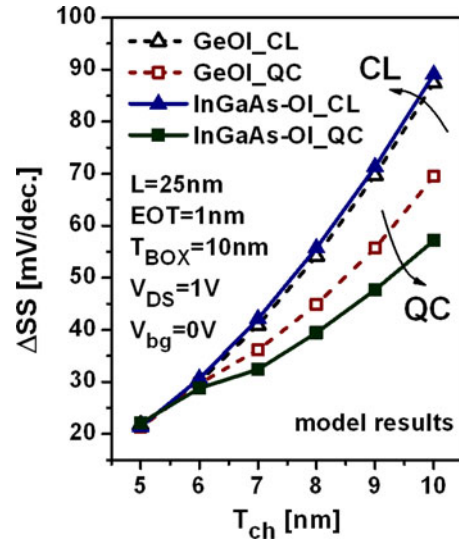


Fig. 7. Impact of channel thickness on the short-channel subthreshold swing shift  $\Delta SS = SS(L) - SS(L = 100 \text{ nm})$  for InGaAs-OI and GeOI devices.

close to that of the SOI devices even at  $L = 25 \text{ nm}$  which means that the SS of GeOI devices has larger improvement than that of the SOI devices. This is because the GeOI device experiences higher degree of quantum confinement than the SOI counterpart due to the smaller quantization effective mass of Ge. The reason why the QC effect improves the subthreshold swing of UTB devices can be explained by Fig. 6, which shows the electron density distribution along the channel thickness direction for the UTB GeOI device with  $T_{ch} = 10 \text{ nm}$ .

It can be seen that the electron conduction path under the classical condition is closer to the backgate interface (BOX/channel interface) than the QC counterpart. Although the use of thin BOX may suppress the buried-insulator-induced-barrier lowering (BIIBL) [18] effect, the electron conduction path of the GeOI device is still far from the frontgate interface because of the high permittivity of Ge channel. However, the quantum-confinement effect moves the carrier centroid toward the frontgate interface so that the subthreshold swing of the UTB GeOI device improves.

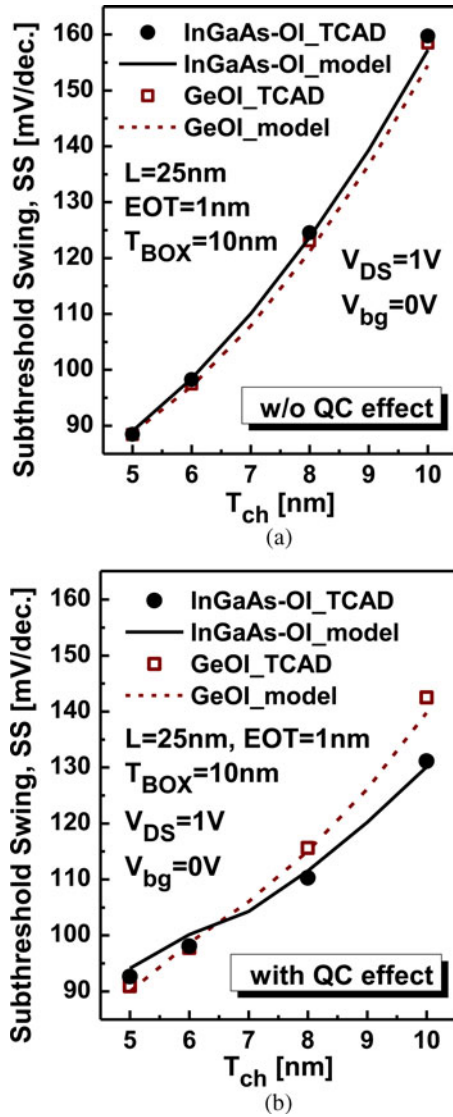


Fig. 8. Comparison of the subthreshold swing for InGaAs-OI and GeOI devices: (a) without the QC effect, i.e., CL condition, and (b) with the QC effect.

#### IV. COMPARISON BETWEEN INGAAS-OI AND GEOI MOSFETS

Fig. 7 compares the impact of quantum confinement on the short-channel subthreshold swing shift ( $\Delta SS = SS(L) - SS(L = 100\text{ nm})$ ) of InGaAs-OI and GeOI devices. It can be seen that the InGaAs-OI devices show comparable classical short-channel subthreshold swing shift to that of the GeOI devices. However, as the QC effect is considered in Fig. 7, the InGaAs-OI devices show better short-channel subthreshold swing shift than the GeOI devices. Fig. 8(a) compares the classical subthreshold swing of UTB InGaAs-OI and GeOI devices for various  $T_{ch}$  with  $L = 25\text{ nm}$ . It can be seen that the InGaAs-OI device with  $T_{ch} = 10\text{ nm}$  has almost the same classical subthreshold swing as the GeOI device for  $V_{DS} = 1\text{ V}$ . However, after considering the QC effect [Fig. 8(b)], the InGaAs-OI device shows better subthreshold swing than the GeOI counterpart. In addition, it

can be seen from Fig. 8(b) that the improvement of SS due to the QC effect for InGaAs devices decreases with decreasing  $T_{ch}$  because of the suppression of drain-field penetration by smaller  $T_{ch}$ . It should be noted that, as indicated in Fig. 2, the InGaAs device possesses a larger ground-state eigen-energy ( $E_0 - E_{C, \min}$ ) than the Ge counterpart and thus higher degree of quantum confinement. This explains why the subthreshold swing of InGaAs-OI devices gains larger improvement than the GeOI counterpart.

#### V. CONCLUSION

We have investigated the subthreshold swing and electrostatic integrity for UTB GeOI and InGaAs-OI n-MOSFETs considering quantum confinement using a derived analytical solution of Schrödinger equation verified with TCAD numerical simulation. Although the electron conduction path of the high-mobility channel device can be far from the frontgate interface due to high channel permittivity, our study indicates that the quantum confinement effect can move the carrier centroid toward the frontgate so that subthreshold swing of the UTB device can improve. Since InGaAs, Ge, and Si channels exhibit different degree of quantum confinement due to different quantization effective mass, the impact of quantum confinement has to be considered when one-to-one comparisons among UTB InGaAs-OI, GeOI, and SOI MOSFETs regarding the subthreshold swing and electrostatic integrity are made.

#### REFERENCES

- [1] M. Radosavljevic, B. Chu-Kung, S. Corcoran, G. Dewey, M. K. Hudait, J. M. Fastenau, J. Kavalieros, W. K. Liu, D. Lubyshev, M. Metz, K. Millard, N. Mukherjee, W. Rachmady, U. Shah, and Robert Chau, "Advanced high-K gate dielectric for high-performance short-channel  $\text{In}_{0.7}\text{Ga}_{0.3}\text{As}$  quantum well field effect transistors on silicon substrate for low power logic applications," in *IEDM Tech. Dig.*, Dec., 2009, pp. 319–322.
- [2] E. Pop, C. O. Chui, S. Sinha, R. Dutton, and K. Goodson, "Electrothermal comparison and performance optimization of thin-body SOI and GOI MOSFETs," in *IEDM Tech. Dig.*, Dec., 2004, pp. 411–414.
- [3] S. W. Bedell, A. Majumdar, J. A. Ott, J. Arnold, K. Fogel, S. J. Koester, and D. K. Sadana, "Mobility scaling in short-channel length strained Ge-on-insulator P-MOSFETs," in *IEEE Electron Device Lett.*, Jul., 2008, vol. 29, no. 7, pp. 811–813.
- [4] F. Andrieu, O. Weber, J. Mazurier, O. Thomas, J.-P. Noel, C. Fenouillet-Béranger, J.-P. Mazerillier, P. Perreau, T. Poiroux, Y. Morand, T. Morel, S. Allegret, V. Loup, S. Barnola, F. Martin, J.-F. Damlencourt, I. Servin, M. Cassé, X. Garros, O. Rozeau, M.-A. Jaud, G. Cibrario, J. Cluzel, A. Toffoli, F. Allain, R. Kies, D. Lafond, V. Delaye, C. Tabone, L. Tosti, L. Brévard, P. Gaud, V. Paruchuri, K. K. Bourdelle, W. Schwarzenbach, O. Bonnin, B.-Y. Nguyen, B. Doris, F. Boeuf, T. Skotnicki, and O. Faynot, "Low leakage and low variability ultra-thin body and buried oxide (UT2B) SOI technology for 20 nm low power CMOS and beyond," in *Proc. 2010 VLSI Symp. Tech. Dig.*, Jun. pp. 57–58.
- [5] C. Fenouillet-Béranger, O. Thomas, P. Perreau, J.-P. Noel, A. Bajolet, S. Haendler, L. Tosti, S. Barnola, R. Beneyton, C. Perrot, C. de Buttet, F. Abbate, F. Baron, B. Pernet, Y. Campidelli, L. Pinzelli, P. Gouraud, O. Faynot, and T. Skotnicki, "Efficient multi-VT FDSOI technology with UTBOX for low power circuit design," in *Proc. 2010 VLSI Symp. Tech. Dig.*, Jun., pp. 65–66.
- [6] Y.-S. Wu, H.-Y. Hsieh, V. P.-H. Hu, and P. Su, "Impact of quantum confinement on short-channel effects for ultrathin-body Germanium-on-insulator MOSFETs," *IEEE Electron Device Lett.*, vol. 32, no. 1, pp. 18–20, Jan. 2011.
- [7] F. Stern and W. E. Howard, "Properties of semiconductor surface inversion layers in the electric quantum limit," *Phys. Rev.*, vol. 163, no. 3, pp. 816–835, Nov. 1967.

- [8] K. H. Goetz, D. Bimberg, H. Jurgensen, J. Selders, A. V. Solomonov, G. F. Glinskii, and M. Razeghi, "Optical and crystallographic properties and impurity incorporation of  $\text{Ga}_x\text{In}_{1-x}\text{As}$  ( $0.44 < x < 0.49$ ) grown by liquid phase epitaxy, vapor phase epitaxy, and metal organic chemical vapor deposition," *J. Appl. Phys.*, vol. 54, no. 8, pp. 4543–4552, 1983.
- [9] V. P. Trivedi and J. G. Fossum, "Quantum-mechanical effects on the threshold voltage of undoped double-gate MOSFETs," *IEEE Electron Device Lett.*, vol. 26, no. 8, pp. 579–582, Aug. 2005.
- [10] Y.-S. Wu and P. Su, "Analytical quantum-confinement model for short-channel gate-all-around MOSFETs under subthreshold region," *IEEE Trans. Electron Devices*, vol. 56, no. 11, pp. 2720–2725, Nov. 2009.
- [11] V. P.-H. Hu, Y.-S. Wu, and P. Su, "Investigation of electrostatic integrity for ultrathin-body Germanium-on-nothing MOSFET," *IEEE Trans. Nanotechnol.*, vol. 10, no. 2, pp. 325–330, Mar. 2011.
- [12] K. K. Young, "Short-channel effect in fully depleted SOI MOSFET's," *IEEE Trans. Electron Devices*, vol. 36, no. 2, pp. 399–402, Feb. 1989.
- [13] D. G. Zill and M. R. Cullen, *Differential Equations With Boundary Value Problems*, 5th ed. Pacific Grove, CA: Brooks/Cole, 2001.
- [14] H. Ananthan and K. Roy, "A compact physical model for yield under gate length and body thickness variations in nanoscale double-gate CMOS," *IEEE Trans. Electron Devices*, vol. 53, no. 9, pp. 2151–2159, Sep. 2006.
- [15] Y.-S. Wu and P. Su, "Sensitivity of gate-all-around nanowire MOSFETs to process variation—A comparison with multigate MOSFETs," *IEEE Trans. Electron Devices*, vol. 55, no. 11, pp. 3042–3047, Nov. 2008.
- [16] X. Liang and Y. Taur, "A 2-D analytical solution for SCEs in DG MOSFETs," *IEEE Trans. Electron Devices*, vol. 51, no. 9, pp. 1385–1391, Sep. 2004.
- [17] *ATLAS User's Manual*, SILVACO, Santa Clara, CA, 2008.
- [18] Y. Omura, H. Konish, and S. Sato, "Quantum-mechanical suppression and enhancement of SCEs in ultrathin SOI MOSFETs," *IEEE Trans. Electron Devices*, vol. 53, no. 4, pp. 677–684, Apr. 2006.



**Chang-Hung Yu** (S'11) was born in Taipei, Taiwan, in 1985. He received the B.S. degree from the Department of Civil Engineering, National Taiwan University, Taipei, Taiwan, in 2007, and the M.S. degree in 2011 from the Department of Electronics Engineering, National Chiao Tung University, Hsinchu, Taiwan, where he is currently working toward the Ph.D. degree at the Institute of Electronics. His current research interests include design and modeling of emerging CMOS devices.



**Yu-Sheng Wu** (S'09) received the B.S. and M.S. degrees in electronics engineering from the Department of Electronics Engineering, National Chiao Tung University, Hsinchu, Taiwan, in 2004 and 2006, respectively, where he is currently working toward the Ph.D. degree at the Institute of Electronics.

His current research interests include design and modeling of advanced CMOS devices.



**Vita Pi-Ho Hu** (S'09) received the B.S. degree from the Department of Materials Science and Engineering, National Chiao Tung University, Hsinchu, Taiwan, in 2004, where she is currently working toward the Ph. D. degree in the Institute of Electronics.

Her research interests include ultralow power SRAM using emerging devices, and the impact of emerging devices on circuit design.



**Pin Su** (S'98–M'02) received the B.S. and M.S. degrees in electronics engineering from National Chiao Tung University, Taiwan, and the Ph.D. degree from the Department of Electrical Engineering and Computer Sciences, University of California at Berkeley.

From 1997 to 2003, he conducted his doctoral and postdoctoral research in Silicon-On-Insulator (SOI) devices at Berkeley. He was also one of the major contributors to the unified BSIMSOI model, the first industrial standard SOI MOSFET model for circuit design. Since August 2003, he has been with the Department of Electronics Engineering, National Chiao Tung University, Taiwan, where he is currently a Full Professor. His research interests include silicon-based nanoelectronics, modeling and design for exploratory CMOS devices, and device/circuit interaction and co-optimization in nano-CMOS. He has authored or coauthored more than 130 research papers in refereed journals and international conference proceedings in these areas.